

# Unleash the Potential of Long Semantic IDs for Generative Recommendation

Ming Xia\*

xiamingtx03@gmail.com

Southern University of Science and Technology  
Shenzhen, China

Guoxin Ma\*

guoxinma9@gmail.com

Xi'an Jiaotong University  
Xian, China

Zhiqin Zhou\*

zinchou0110@gmail.com

Nanjing university  
suzhou, China

Dongmin Huang†

dmhuang777@gmail.com

Southern University of Science and Technology  
Shenzhen, China

## ABSTRACT

Semantic ID-based generative recommendation represents items as sequences of discrete tokens, but it inherently faces a trade-off between representational expressiveness and computational efficiency. Residual Quantization (RQ)-based approaches restrict semantic IDs to be short to enable tractable sequential modeling, while Optimized Product Quantization (OPQ)-based methods compress long semantic IDs through naive rigid aggregation, inevitably discarding fine-grained semantic information. To resolve this dilemma, we propose ACERec, a novel framework that decouples the granularity gap between fine-grained tokenization and efficient sequential modeling. It employs an Attentive Token Merger to distill long expressive semantic tokens into compact latents and introduces a dedicated Intent Token serving as a dynamic prediction anchor. To capture cohesive user intents, we guide the learning process via a dual-granularity objective, harmonizing fine-grained token prediction with global item-level semantic alignment. Extensive experiments on six real-world benchmarks demonstrate that ACERec consistently outperforms state-of-the-art baselines, achieving an average improvement of 14.40% in NDCG@10, effectively reconciling semantic expressiveness and computational efficiency.

## CCS CONCEPTS

• Information systems → Recommender systems.

## KEYWORDS

Semantic ID; Sequential Recommendation

## 1 INTRODUCTION

Generative recommendation has recently emerged as a paradigm shift, moving the field beyond the conventional “retrieve-then-rank” pipeline toward a direct generation approach [19, 30, 31]. Conventional item ID-based recommendation models assign each item an arbitrary unique identifier [16, 38], relying on a dedicated embedding table which scales linearly with the catalog [14]. This design incurs substantial memory overhead and constrains scalability, while also modeling items as isolated symbols without explicit semantic structure. As a result, such models are prone to

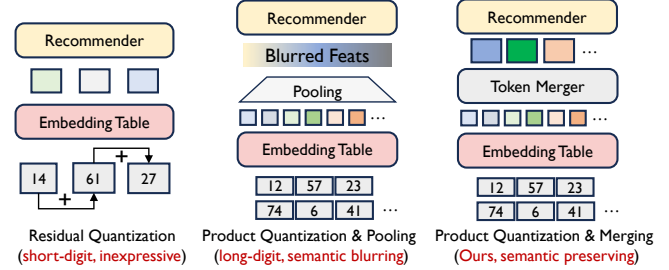


**Figure 1: Comparison of representation paradigms.** Left: RQ (short/serial codes) with limited expressiveness. Middle: PQ + pooling causes semantic blurring. Right: ACERec merges long semantic tokens for expressiveness and efficiency.

cold-start and data sparsity challenges: unseen or rarely interacted items lack informative representations and cannot effectively benefit from knowledge transfer across the catalog. In contrast, generative approaches represent each item as a sequence of discrete semantic tokens drawn from a shared vocabulary (*i.e.*, codebooks). This shared tokenization embeds all items into a unified semantic space, where common attributes and patterns are encoded by reusable tokens rather than isolated item IDs. Consequently, these models can generalize semantics across items and transfer knowledge through shared tokens, enabling them to track how user preferences evolve along behavior sequences and to infer complex intents beyond surface-level co-occurrence [11, 25].

Despite their promise, existing generative recommenders predominantly rely on Residual Quantization (RQ) [35] to construct hierarchical semantic IDs. However, the strict serial dependency [10] of RQ forces practical systems to limit code lengths (*e.g.*, 3–4 tokens) to satisfy latency budgets, inevitably sacrificing representational expressiveness and fine-grained semantic resolution [20, 25]. In contrast, Optimized Product Quantization (OPQ) [6, 15] breaks this bottleneck via orthogonal subspace decomposition. This design decouples codebook dependencies, enabling parallel generation and supporting much longer semantic IDs (*e.g.*, 32 tokens) for richer item representation [11, 12]. Yet, this expressiveness comes at a steep cost: directly feeding long semantic-ID sequences into Transformer-based [29] recommenders creates a prohibitive computational burden. With  $L$  historical items and  $m$  tokens per item, the effective input length explodes to  $N=L \times m$ , incurring a

\*Equal contribution.

†Corresponding authors.

quadratic self-attention complexity of  $O(N^2)$  that severely hampers training and inference efficiency.

To alleviate the efficiency bottleneck of OPQ, recent works resort to aggregating the long token sequence into a unified vector (e.g., via mean pooling) [11, 12]. While this restores efficiency, such rigid aggregation inevitably causes semantic blurring, as it erodes fine-grained intra-item patterns and conflates distinct semantic attributes originating from different orthogonal spaces. This creates a paradox between representation and utilization, where long semantic IDs are introduced to encode rich and fine-grained semantics, yet the recommender ultimately consumes a degraded summary that discards details OPQ was designed to capture. The differences between these paradigms are illustrated in Figure 1. In this work, we pose a critical question: Can we retain the full semantic richness of long IDs while achieving high inference efficiency, without resorting to lossy averaging? We argue that the solution lies in decoupling tokenization granularity from the recommendation process, avoiding the forced choice between computationally expensive raw sequences and over-compressed pooled vectors, and enabling efficient recommendation without sacrificing semantic fidelity.

Based on this insight, we propose ACERec (Adaptive Compression for Efficient Recommendation), a framework that bridges high-capacity semantic representations and efficient sequential modeling. Instead of sacrificing OPQ’s expressive capacity or directly feeding excessively long token sequences into the recommender, ACERec introduces an Attentive Token Merger (ATM) to adaptively compress long semantic IDs into fixed-size latents. Specifically, ATM maintains a small set of learnable latent queries (e.g., 4), which attend to the original token sequence (e.g., 32) and aggregate salient semantics into compact latent tokens. By replacing rigid averaging with content-adaptive aggregation, ATM preserves fine-grained intra-item semantic structure while keeping the computational cost tractable. To orchestrate the sequential modeling for generative next-item recommendation over these multi-token representations, ACERec features a dedicated Intent Token, which aggregates historical context and functions as a dynamic query for next-item generation. Crucially, to capture the essence of user intents, we propose a dual-granularity optimization strategy that combines token-wise supervision for parallel generation [8] with item-wise semantic alignment between the Intent Token and the target item’s summary embedding, providing complementary constraints on both precise token prediction and holistic semantic intent.

To summarize, our main contributions are as follows:

- We propose ACERec, a novel framework that decouples the granularity of semantic tokenization from sequential recommendation, enabling the expressiveness of long semantic IDs while keeping computation tractable.
- We introduce an intent-centric prediction anchor with dual-level supervision, which alleviates anchor ambiguity and consistently improves next-item recommendation performance while preserving efficient parallel decoding.
- ACERec achieves state-of-the-art performance on multiple benchmarks, yielding an average of 14.40% improvement in NDCG@10. Further cold-start analysis shows its advantage in leveraging fine-grained semantic knowledge.

## 2 METHODOLOGY

In this section, we introduce ACERec, a recommendation framework that decouples the semantic granularity of tokenization from the computation budget of sequential modeling. We first formulate the sequential recommendation task (Section 2.1). Next, we introduce the tokenization and compression process, where we quantize items into semantic tokens and distill token embeddings to compact latents (Section 2.2). We then explain how ACERec aggregates user intents (Section 2.3) and achieves efficient recommendation inference (Section 2.4). Finally, we discuss the connections and distinctions between ACERec and existing paradigms (Section 2.5).

The overall architecture of ACERec is illustrated in Figure 2. In addition, we summarize the complete training and inference pipelines in Algorithm 1 and Algorithm 2, with detailed algorithmic steps provided in Appendix B.

### 2.1 Sequential Recommendation Task

Let  $\mathcal{U}$  and  $\mathcal{I}$  denote the set of users and items, respectively. For each user  $u \in \mathcal{U}$ , the interaction history is represented as a chronological sequence  $\mathcal{S}_u = \{i_1, i_2, \dots, i_L\}$ . The goal of sequential recommendation is to predict the next item  $i_{L+1}$  from the candidate set  $\mathcal{I}$  [16, 27]. This can be formulated as learning a conditional distribution  $P(i_{L+1} | \mathcal{S}_u)$ .

In the paradigm of Generative Sequential Recommendation, each item  $i$  is represented not by an atomic ID, but by a sequence of  $m$  discrete tokens (i.e., semantic IDs), denoted as  $\mathbf{c}_i = (c_{i,1}, c_{i,2}, \dots, c_{i,m})$ . Consequently, the recommendation task is reformulated as generating the token sequence of the target item given the user’s history [12, 25]. Two decoding strategies exist for this generation process: (1) *Autoregressive Decoding*: Early approaches [20, 25] flatten the history into a long stream and generate tokens step-by-step via beam search [10], modeling the conditional probability  $P(c_{i,k} | c_{i,<k}, \mathcal{S}_u)$ . (2) *Parallel Decoding*: Recent methods [11, 12] utilize OPQ [6, 15], which decomposes item embeddings into orthogonal subspaces. This structure supports a conditional independence assumption, enabling the parallel prediction of all  $m$  tokens, i.e.  $P(\mathbf{c}_{i_{L+1}} | \mathcal{S}_u) \approx \prod_{k=1}^m P(c_{i_{L+1},k} | \mathcal{S}_u)$ .

### 2.2 Tokenization and Compression

To fully leverage the rich expressive power of long semantic sequences while meeting the efficiency requirements of sequential recommendation, we propose a two-step input processing pipeline: *OPQ-based Tokenization* followed by *Attentive Token Merging*.

**2.2.1 Semantic Tokenization via OPQ.** We adopt OPQ to represent items as discrete semantic IDs. It maps each item  $i$  into a code tuple  $(c_1, \dots, c_m)$ . Specifically, it decomposes the item embedding into  $m$  orthogonal subspaces, where the  $k$ -th token  $c_k$  is quantized using a specific codebook  $C^{(k)}$ . This orthogonal decomposition largely disentangles semantic attributes across digits, supporting the assumption of conditional independence for parallel prediction.

To capture rich item details, we maintain a large tuple length (e.g.,  $m = 32$ ). Each discrete token  $c_k$  is then projected into a dense vector via a learnable embedding table, yielding the semantic embedding sequence  $\mathbf{E}_i = (\mathbf{e}_1, \dots, \mathbf{e}_m) \in \mathbb{R}^{m \times d}$ .

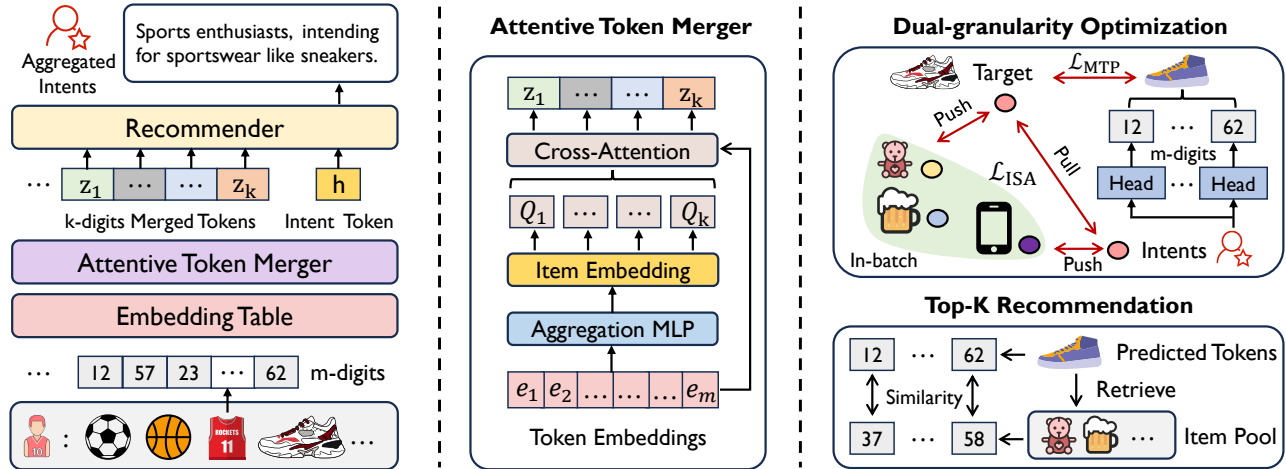


Figure 2: Overview architecture of ACERec. The left panel illustrates the sequence encoding process, where historical items are tokenized and distilled into compact latents, then aggregated into user intents. The middle panel details ATM, which employs cross-attention to adaptively filter subspace signals into latent representations (Section 2.2). The right panel displays the training and inference paradigms: the upper part depicts the dual-granularity optimization (Section 2.3), while the lower part demonstrates the holistic candidate scoring strategy for efficient parallel retrieval (Section 2.4).

2.2.2 *Latent Token Distillation via ATM*. To resolve the conflict between the high semantic expressiveness and sequential recommendation efficiency, we introduce ATM, which employs a content-adaptive aggregation mechanism to compress the long semantic sequence into a compact set of latent tokens.

**Content-adaptive Latent Query Generation.** First, to guide the extraction of diverse semantic features, we generate  $k$  content-adaptive queries. Specifically, we aggregate the token embeddings into a holistic summary vector  $s_i$  via a nonlinear projection  $f_s$ , and then transform it into  $k$  distinct query vectors  $Q_i \in \mathbb{R}^{k \times d}$  via query projector  $f_q$ :

$$\begin{aligned} s_i &= f_s(e_1, \dots, e_m), \\ Q_i &= f_q(s_i). \end{aligned} \quad (1)$$

These adaptive queries are conditioned on the specific item content, enabling the merger to focus on different semantic aspects for each item.

**Attentive Token Merging.** Next, we illustrate the merging process. To preserve the subspace identity of the OPQ digits, we inject learnable positional embeddings  $P \in \mathbb{R}^{m \times d}$  into the raw sequence:  $\tilde{E}_i = E_i + P$ . We then feed the queries  $Q_i$  and inputs  $\tilde{E}_i$  into a multi-head cross-attention layer to produce the latent tokens  $Z_i \in \mathbb{R}^{k \times d}$ , effectively reducing the sequence complexity from  $m$  to  $k$  while retaining critical semantic details:

$$Z_i = f_{out} \left( f_{attn} \left( Q_i, \tilde{E}_i, \tilde{E}_i \right) \right), \quad (2)$$

Here,  $f_{attn}$  performs the cross-attention operation using  $Q_i$  as queries and  $\tilde{E}_i$  as keys/values, while  $f_{out}$  encapsulates the subsequent processing layers (e.g., multi-layer perceptron (MLP)).

### 2.3 Intent-Centric Sequential Modeling

2.3.1 *Modeling Evolving User Intent*. Sequential recommendation aims to infer a user’s evolving intent from historical interactions

and leverage it to predict the next item. After attentive compression, each item at step  $t$  is represented as a set of semantic latents  $Z_t = \{z_{t,1}, \dots, z_{t,k}\}$ , which capture complementary item attributes but do not directly form a unified intent representation. To explicitly represent user intent in sequential modeling, we introduce a dedicated *Intent Token* that acts as a central aggregation point for next-item generation.

**Intent Token Formulation.** At each step  $t$ , we append a learnable Intent Token  $h_t \in \mathbb{R}^d$  to the latent set  $Z_t$  and initialize it with the item-level summary  $s_t$  (Eq. 1). The resulting composite representation is denoted as  $\tilde{Z}_t = [Z_t; h_t] \in \mathbb{R}^{(k+1) \times d}$ . The sequential input is then constructed by concatenating all composite steps along the temporal dimension, i.e.,  $H = [\tilde{Z}_1, \tilde{Z}_2, \dots, \tilde{Z}_L]$ .

Unlike semantic latents that explicitly encode item attributes, the Intent Token does not represent the item itself but serves as a context-conditioned state that aggregates semantic evidence for intent modeling.

**Step-wise Causal Attention.** To model both semantic coherence within items and temporal dependency across interactions, we employ a step-wise causal attention mechanism over the sequence  $H = [\tilde{Z}_1, \dots, \tilde{Z}_L]$ , where each step  $\tilde{Z}_t = [Z_t; h_t]$  corresponds to one user-item interaction.

The attention mask enforces causality at the interaction level: tokens at step  $t$  are allowed to attend to all tokens from earlier steps  $\tilde{Z}_{<t}$ , while attention to future steps is strictly prohibited. Within the same step, semantic latents  $Z_t$  attend to each other bidirectionally to preserve intra-item semantic consistency, whereas the Intent Token  $h_t$  is permitted to attend to both  $Z_t$  and all tokens from previous steps.

Under this design, the Intent Token  $h_t$  aggregates contextualized semantic evidence across interactions and serves as a dynamic anchor for next-item prediction.

**2.3.2 Dual-Granularity Alignment.** To effectively train the dynamic intent-centric prediction anchor, we adopt a dual-granularity training objective: fine-grained token prediction ensures precise semantic ID generation, while item-level semantic alignment guides the intent representation by focusing it on target-related semantics.

**Fine-grained Token Prediction.** We adopt the MTP objective [8] to enforce exact reconstruction of the semantic IDs of the next item from the predicted intent state. Let  $\mathbf{h}_{\text{pred}} \in \mathbb{R}^d$  denote the final representation of the Intent Token used for prediction. To align with the metric structure induced by product quantization,  $\mathbf{h}_{\text{pred}}$  is first normalized and then projected into  $m$  independent subspace representations  $\{\mathbf{h}_{\text{pred}}^{(k)}\}_{k=1}^m$  via distinct projection heads.

For each digit  $k$ , the probability of predicting the  $v$ -th codeword in the  $k$ -th codebook  $\mathbf{C}^{(k)}$  is computed by scaled dot-product:

$$P(c_k = v \mid \mathbf{h}_{\text{pred}}) = \frac{\exp(\mathbf{h}_{\text{pred}}^{(k)\top} \mathbf{e}_v^{(k)} / \gamma)}{\sum_{v'=1}^M \exp(\mathbf{h}_{\text{pred}}^{(k)\top} \mathbf{e}_{v'}^{(k)} / \gamma)}, \quad (3)$$

where  $\mathbf{e}_v^{(k)}$  denotes the embedding of the  $v$ -th codeword in the  $k$ -th subspace,  $M$  is the codebook size, and  $\gamma$  is a temperature parameter. The MTP loss is defined as the average negative log-likelihood across all  $m$  digits:

$$\mathcal{L}_{\text{MTP}} = -\frac{1}{m} \sum_{k=1}^m \log P(c_{tgt,k} \mid \mathbf{h}_{\text{pred}}), \quad (4)$$

where  $c_{tgt,k}$  is the ground-truth codeword index at the  $k$ -th position.

**Intent-Semantic Alignment (ISA).** While MTP provides fine-grained token-level supervision, its uniform exact-match penalty overlooks the unequal semantic contribution of quantized subspaces, potentially diluting informative signals with low-impact details. To address this, we introduce Intent-Semantic Alignment (ISA), which aligns the predicted intent representation  $\mathbf{h}_i$  with the holistic summary embedding  $\mathbf{s}_{L+1}$  of the target item, guiding the Intent Token to focus on target-relevant semantics.

However, standard in-batch contrastive learning is susceptible to *popularity bias*, as frequently occurring items are over-represented as negatives and thus overly penalized. Following prior work on logit adjustment [1, 2, 33], we adopt a debiased scoring function:

$$\phi(\mathbf{h}_i, \mathbf{s}_j) = \text{sim}(\mathbf{h}_i, \mathbf{s}_j) / \tau - \beta \log P(j), \quad (5)$$

where  $\text{sim}(\cdot, \cdot)$  denotes cosine similarity,  $\tau$  is a temperature parameter,  $P(j)$  is the empirical sampling probability of item  $j$  in the batch, and  $\beta$  controls the strength of the popularity correction. This adjustment discourages trivial alignment driven by item frequency rather than semantic relevance.

The ISA loss is defined as a softmax over the debiased scores:

$$\mathcal{L}_{\text{ISA}} = -\log \frac{\exp(\phi(\mathbf{h}_i, \mathbf{s}_{L+1}))}{\sum_{j \in \mathcal{B}} \exp(\phi(\mathbf{h}_i, \mathbf{s}_j))}, \quad (6)$$

where  $\mathcal{B}$  denotes the set of items in the current batch. This formulation encourages semantic grounding of the intent representation while explicitly mitigating popularity bias.

**Joint Objective.** The final training objective integrates fine-grained exactness and item-level semantic grounding:

$$\mathcal{L} = \mathcal{L}_{\text{MTP}} + \lambda \mathcal{L}_{\text{ISA}}, \quad (7)$$

where  $\lambda$  controls the strength of the intent-semantic alignment regularization.

## 2.4 Efficient Inference via Holistic Scoring

During inference, we employ a *holistic candidate scoring* strategy [15] to perform exact retrieval over the entire item pool  $\mathcal{I}$ . Unlike traditional dense retrieval that requires heavy dot-products for every candidate [16, 27], our approach decouples probability computation from item scoring, executing in two efficient vectorized steps:

**Parallel Subspace Matching.** First, we compute the probability distributions over all  $m$  codebooks. The aggregated intent  $\mathbf{h}_{\text{pred}}$  is projected into  $m$  subspace queries  $\{\mathbf{h}_{\text{pred}}^{(1)}, \dots, \mathbf{h}_{\text{pred}}^{(m)}\}$ . We then calculate the log-probability of the  $v$ -th codeword in the  $k$ -th subspace, denoted as  $\mathbf{P}[k, v]$ , via parallel dot-products with the codebook embeddings  $\mathbf{e}_v^{(k)}$ :

$$\mathbf{P}[k, v] = \log \frac{\exp(\mathbf{h}_{\text{pred}}^{(k)\top} \mathbf{e}_v^{(k)} / \gamma)}{\sum_{v'=1}^M \exp(\mathbf{h}_{\text{pred}}^{(k)\top} \mathbf{e}_{v'}^{(k)} / \gamma)}, \quad (8)$$

where  $\gamma$  is the temperature. Crucially, the computational cost of this step scales with the vocabulary size ( $m \times M$ ), which is independent of the candidate pool size  $|\mathcal{I}|$ .

**Vectorized Score Gathering.** Second, we compute scores for all candidates. Since each item  $j \in \mathcal{I}$  is represented by a pre-quantized token tuple  $\mathbf{c}_j = (c_{j,1}, \dots, c_{j,m})$ , we do not perform further embedding computations. Instead, we treat item IDs as indices to directly retrieve their corresponding log-probabilities from matrix  $\mathbf{P}$  via a fast vectorized gather operation:

$$\text{Score}(j) = \sum_{k=1}^m \mathbf{P}[k, c_{j,k}]. \quad (9)$$

This transforms candidate scoring into a high-speed memory lookup-and-sum process, enabling ACERec to rank items with minimal latency.

## 2.5 Discussion

In this section, we provide an in-depth discussion on the connections and distinctions between ACERec and existing paradigms, followed by a theoretical analysis of computational complexity.

**2.5.1 Comparison with Generative Baselines.** ACERec evolves from existing generative recommenders by explicitly resolving the “Granularity Mismatch” dilemma.

- **vs. TIGER:** Unlike TIGER [25], which couples code length with inference latency due to serial decoding dependencies, ACERec decouples them by leveraging long IDs ( $m \geq 32$ ) for expressive representation but distills them into compact latents ( $k = 4$ ) for efficiency.
- **vs. RPG:** Compared to RPG [12], which suffers from semantic blurring due to rigid mean pooling, ACERec adaptively filters and distills high-density information based on item context, preserving intra-item structures.

**2.5.2 Complexity and Efficiency.** Let  $L$  be the sequence length,  $d$  the dimension. TIGER flattens all  $n$  tokens per item, incurring  $O(L^2 n^2 d)$  self-attention complexity, which is prohibitive for expressive IDs. RPG aggregates tokens into a single vector, reducing complexity to  $O(L^2 d)$  at the cost of information loss. ACERec introduces a linear cost of  $O(L m k d)$  for ATM distillation, while the Transformer

backbone operates on  $N = L \times (k + 1)$  tokens, resulting in  $O(L^2 k^2 d)$  complexity.

Since  $k \ll m$ , ACERec achieves a favorable trade-off: its complexity is significantly lower than modeling the raw sequence ( $k^2 \ll m^2$ ) and retains fine-grained semantics. Regarding inference, ACERec avoids TIGER’s serial bottleneck and RPG’s approximate graph decoding (which requires non-trivial hyperparameter tuning and iterative traversal) by employing fully parallel, exact *holistic scoring* via matrix broadcasting.

### 3 EXPERIMENT

In this section, we conduct extensive experiments on six real-world datasets to answer the following research questions:

- **RQ1:** How does ACERec perform compared with strong discriminative and generative recommendation baselines?
- **RQ2:** How do ACERec’s components contribute to overall performance?
- **RQ3:** Does ACERec effectively decouple tokenization granularity from recommendation efficiency by outperforming direct modeling with short semantic IDs (e.g., 4 tokens) through learned compression of long semantic IDs (e.g., 32 tokens)?

#### 3.1 Experimental Setup

**3.1.1 Datasets.** To comprehensively evaluate the performance of ACERec, we conduct experiments on six datasets from the Amazon Reviews collection [23], covering diverse domains with varying scales, including Sports, Beauty, Toys, Instruments, Office, and Baby. Following prior generative recommendation works [11, 12, 25], user interactions are sorted chronologically and split using a leave-last-out strategy: the last interaction for testing, the second-to-last for validation, and the rest for training. Dataset statistics are provided in Appendix A.3.

**3.1.2 Baselines.** We evaluate the performance of ACERec by comparing it with comprehensive item ID-based and semantic ID-based baselines. Specifically, the **item ID-based methods** include HGN [22], SASRec [16], S<sup>3</sup>-Rec [38], ICLRec [4], and ELCRec [21], while the **semantic ID-based methods** include TIGER [25], ActionPiece [13], ETEGRec [20], and RPG [12]. Detailed descriptions of all baselines are provided in Appendix A.1.

**3.1.3 Evaluation Metrics and Implementation Details.** We adopt full candidate ranking for evaluation, where the ground-truth item is ranked against the entire item set to ensure a rigorous and unbiased assessment. Performance is measured using Recall@ $K$  and NDCG@ $K$  with  $K \in \{5, 10\}$ . We load the model with the highest validation NDCG@10 for testing. Implementation details and hyperparameter settings are provided in Appendix A.2.

#### 3.2 Overall Performance (RQ1)

Table 1 and Table 2 report the overall performance on six benchmarks. ACERec achieves the best results across all datasets and metrics, improving over the strongest baseline in NDCG@10 by 15.70% on Sports, 14.91% on Beauty, and 22.15% on Toys.

The results also lead to three observations. First, semantic ID-based generative methods generally outperform item ID-based baselines, demonstrating stronger knowledge transfer via shared

semantic tokens and better generalization across items. Second, this advantage is not always consistent, as strong item ID-based intent-learning models such as ELCRec remain highly competitive and even outperform some semantic baselines on several datasets, suggesting that current semantic ID-based approaches may not fully translate token semantics into intent modeling gains. Third, Instruments stands out as a difficult dataset for existing semantic ID-based methods, yet ACERec delivers large improvements over RPG, with 58.11% and 55.93% relative gains in Recall@5 and NDCG@5, respectively, indicating that ACERec better unleashes the potential of long semantic IDs in challenging settings.

#### 3.3 Ablation Study of ACERec (RQ2)

In this part, we conduct a comprehensive ablation study to dissect the architecture of ACERec. We structure the analysis in two parts: (1) **Component Contribution**, where we progressively evolve the baseline to isolate the gains from ATM, the Intent Token, and the ISA loss; and (2) **Architectural Design Analysis**, where we conduct fine-grained comparisons to validate our specific choices for the *merging strategy* (input compression) and *generation anchor* (output aggregation).

**3.3.1 Impact of Key Components.** To ensure a fair comparison, we adopt RPG equipped with holistic scoring as the starting baseline (Row 1).

- **Individual Efficacy of ATM and Intent Token (Row 2 & 3):** Incorporating either ATM or the Intent Token yields substantial improvements over the baseline. Specifically, ATM (Row 2) boosts Recall@10 on Instruments by 21% (0.0826  $\rightarrow$  0.1001), confirming that preserving fine-grained semantics via attentive resampling is superior to rigid mean pooling. Similarly, the Intent Token (Row 3) outperforms the baseline by providing a dynamic anchor for sequence modeling.
- **Impact of Intent-Semantic Alignment (Row 3 vs. 4):** A key observation is the comparison between Row 3 and Row 4. Even without the high-fidelity input from ATM, adding the  $\mathcal{L}_{ISA}$  objective to the Intent Token model brings a clear gain (e.g., Instruments Recall@10 improves from 0.0994 to 0.1064). This verifies that the semantic alignment regularization works independently of the input granularity, successfully guiding the model to capture salient item features (holistic summary) rather than just fitting token IDs.
- **Synergy in the Full Model (Row 5 & 6):** When ATM and the Intent Token are combined (Row 5), the performance leaps significantly (Recall@10 reaches 0.1162), demonstrating their strong complementarity: ATM ensures high-quality input, while the Intent Token ensures precise aggregation. Finally, applying  $\mathcal{L}_{ISA}$  to this combined architecture (Row 6) achieves the best overall performance (0.1190). This confirms that our dual-granularity optimization, which combines fine-grained token prediction (MTP) with global semantic alignment (ISA), effectively unlocks the potential of semantic IDs.

**3.3.2 Ablation of Architectural Designs.** Beyond validating the overall framework, we further examine whether our specific

**Table 1: Performance comparison of ACERec and baselines on four benchmark datasets. The best and second-best results are denoted in bold and underline, respectively. The “Improv.” row indicates the percentage improvement of ACERec over the strongest baseline.**

Model	Sports				Beauty				Toys				Instruments			
	R@5	N@5	R@10	N@10												
<i>Item ID-based</i>																
HGN	0.0189	0.0120	0.0313	0.0159	0.0325	0.0206	0.0512	0.0266	0.0321	0.0221	0.0497	0.0277	0.0550	0.0442	0.0867	0.0559
SASRec	0.0233	0.0154	0.0350	0.0192	0.0387	0.0249	0.0605	0.0318	0.0463	0.0306	0.0675	0.0374	0.0476	0.0242	0.0840	0.0360
S <sup>3</sup> -Rec	0.0251	0.0161	0.0385	0.0204	0.0387	0.0244	0.0647	0.0327	0.0443	0.0294	0.0700	0.0376	0.0679	0.0420	0.1148	0.0570
ICLRec	0.0274	0.0179	0.0426	0.0228	0.0488	0.0322	0.0739	0.0403	0.0573	0.0395	0.0812	0.0472	0.0539	0.0374	0.0938	0.0503
ELCRec	0.0276	0.0180	0.0414	0.0225	0.0502	0.0351	0.0727	0.0423	0.0580	0.0398	0.0815	0.0474	0.0693	0.0467	0.1155	0.0617
<i>Semantic ID-based</i>																
TIGER	0.0264	0.0181	0.0400	0.0225	0.0454	0.0321	0.0648	0.0384	0.0521	0.0371	0.0712	0.0432	0.0552	0.0368	0.0831	0.0457
ETEGRec	0.0248	0.0159	0.0404	0.0209	0.0420	0.0271	0.0668	0.0350	0.0445	0.0286	0.0716	0.0373	0.0616	0.0417	0.0903	0.0509
ActionPiece	0.0285	0.0187	<u>0.0441</u>	0.0238	0.0484	0.0322	<u>0.0762</u>	0.0412	0.0473	0.0310	0.0725	0.0391	0.0630	0.0407	0.0917	0.0501
RPG	<u>0.0292</u>	<u>0.0196</u>	0.0435	<u>0.0242</u>	<u>0.0512</u>	<u>0.0355</u>	0.0757	<u>0.0436</u>	0.0557	0.0384	0.0777	0.0454	0.0518	0.0354	0.0854	0.0458
<b>ACERec</b>	<b>0.0341</b>	<b>0.0231</b>	<b>0.0493</b>	<b>0.0280</b>	<b>0.0591</b>	<b>0.0421</b>	<b>0.0841</b>	<b>0.0501</b>	<b>0.0688</b>	<b>0.0505</b>	<b>0.0916</b>	<b>0.0579</b>	<b>0.0819</b>	<b>0.0552</b>	<b>0.1211</b>	<b>0.0674</b>
<b>Improv.</b>	+16.78%	+17.86%	+11.79%	+15.70%	+15.43%	+18.59%	+10.37%	+14.91%	+18.62%	+26.88%	+12.39%	+22.15%	+18.18%	+18.20%	+4.85%	+9.24%

**Table 2: Performance comparison on the Office and Baby datasets. The notations follow Table 1.**

Model	Office				Baby			
	R@5	N@5	R@10	N@10	R@5	N@5	R@10	N@10
<i>Item ID-based</i>								
HGN	0.0342	0.0303	0.0580	0.0389	0.0159	0.0122	0.0278	0.0167
SASRec	0.0493	0.0255	0.0881	0.0379	0.0114	0.0058	0.0212	0.0089
S <sup>3</sup> -Rec	<u>0.0587</u>	<u>0.0381</u>	<u>0.0989</u>	<u>0.0509</u>	0.0246	0.0159	0.0410	0.0211
ICLRec	0.0516	0.0342	0.0822	0.0440	0.0250	0.0163	0.0401	0.0211
ELCRec	0.0481	0.0157	0.0728	0.0403	0.0247	0.0157	0.0406	0.0209
<i>Semantic ID-based</i>								
TIGER	0.0359	0.0224	0.0607	0.0303	0.0160	0.0101	0.0260	0.0133
ETEGRec	0.0336	0.0216	0.0612	0.0304	0.0138	0.0084	0.0246	0.0118
ActionPiece	0.0512	0.0334	0.0858	0.0444	<u>0.0269</u>	<u>0.0175</u>	<u>0.0424</u>	<u>0.0225</u>
RPG	0.0579	0.0381	0.0917	0.0490	0.0254	0.0174	0.0394	0.0220
<b>ACERec</b>	<b>0.0683</b>	<b>0.0471</b>	<b>0.1023</b>	<b>0.0579</b>	<b>0.0301</b>	<b>0.0208</b>	<b>0.0427</b>	<b>0.0249</b>
<b>Improv.</b>	+16.35%	+23.62%	+3.44%	+13.75%	+11.90%	+18.86%	+0.71%	+10.67%

**Table 3: Ablation analysis of ACERec components.**

Components		Instruments				Office				
ATM	Intent	ISA	R@5	N@5	R@10	N@10	R@5	N@5	R@10	N@10
✗	✗	✗	0.0490	0.0343	0.0826	0.0448	0.0587	0.0386	0.0928	0.0496
✓	✗	✗	0.0644	0.0429	0.1001	0.0545	0.0661	0.0451	0.0954	0.0545
✗	✓	✗	0.0623	0.0413	0.0994	0.0531	0.0640	0.0433	0.0993	0.0546
✗	✓	✓	0.0658	0.0452	0.1064	0.0582	0.0626	0.0421	0.0991	0.0537
✓	✓	✗	0.0770	0.0527	0.1162	0.0653	0.0669	0.0463	0.0970	0.0559
✓	✓	✓	<b>0.0819</b>	<b>0.0552</b>	<b>0.1211</b>	<b>0.0674</b>	<b>0.0683</b>	<b>0.0471</b>	<b>0.1023</b>	<b>0.0579</b>

architectural choices are necessary. We therefore conduct fine-grained ablations on (i) the merging strategy and (ii) the generation anchor, as reported in Table 4.

**Table 4: Fine-grained ablation of architectural designs.**

Model	Instruments				Office			
	R@5	N@5	R@10	N@10	R@5	N@5	R@10	N@10
<i>Ablation of Merging Strategies</i>								
MLP	0.0756	0.0504	0.1085	0.0606	0.0667	0.0453	0.1013	0.0564
Mean-Pooling	0.0742	0.0502	0.1106	0.0618	0.0656	0.0445	0.0985	0.0549
Convolution	0.0756	0.0501	0.1190	0.0640	0.0648	0.0443	0.1007	0.0558
ATM	<b>0.0819</b>	<b>0.0552</b>	<b>0.1211</b>	<b>0.0674</b>	<b>0.0683</b>	<b>0.0471</b>	<b>0.1023</b>	<b>0.0579</b>
<i>Ablation of Generation Anchor</i>								
Last-Token	0.0644	0.0429	0.1001	0.0545	0.0661	0.0451	0.0954	0.0545
Mean-Pooling	0.0665	0.0476	0.0994	0.0580	0.0616	0.0414	0.0952	0.0522
MLP	0.0665	0.0454	0.1001	0.0560	0.0638	0.0439	0.0946	0.0537
Intent-Token	<b>0.0770</b>	<b>0.0527</b>	<b>0.1162</b>	<b>0.0653</b>	<b>0.0669</b>	<b>0.0463</b>	<b>0.0970</b>	<b>0.0559</b>

- **Impact of Merging Strategy.** We replace ATM with MLP, Mean Pooling, and Convolution while keeping the rest unchanged. ATM consistently achieves the best performance across datasets and metrics. Notably, although convolutional merging can yield competitive recall in some cases, it remains inferior in NDCG, indicating weaker ranking precision. This pattern suggests that *how* information is preserved matters: rigid aggregations (MLP/Pooling) compress long OPQ sequences into a fixed summary in an indiscriminate manner, which tends to dilute discriminative cues. In contrast, ATM leverages cross-attention to adaptively select and aggregate content-dependent subspace signals, distilling the semantics most relevant for downstream intent modeling and ranking into compact latent tokens.
- **Impact of Generation Anchor Strategy.** We compare our Intent Token with three conventional ways to obtain a prediction anchor from the last item’s latent set  $Z_L$ : *Last-Token*, *Mean-Pooling*, and *MLP* over the last-item tokens. As shown in Table 4 (lower), Intent-Token consistently outperforms static anchors, e.g., on Instruments, it improves Recall@10 from

0.1001 to 0.1162 and NDCG@10 from 0.0545 to 0.0653. This gain validates the necessity of our intent-centric design over traditional passive aggregation. Static anchors treat latents as a fixed bag of features without canonical ordering, inevitably leading to either critical information discard (Last-Token) or “semantic blurring” (Pooling/MLP). In contrast, empowered by step-wise causal attention, the Intent Token acts as a proactive, context-conditioned aggregator. It dynamically queries relevant semantic evidence from historical latents, effectively orchestrating complementary item attributes into a cohesive representation of the evolving interest.

### 3.4 Analysis of Tokenization Granularity (RQ3)

A core premise of ACERec is that decoupling the tokenization granularity from the recommendation efficiency is essential. In this section, we investigate this hypothesis by analyzing the impact of compression ratios and comparing our learned compression against direct short tokenization.

**3.4.1 Impact of Compression Ratio.** We investigate the compression ratio  $r = m/k$ , by varying it within  $\{2, 4, 8, 16\}$ . As shown in Figure 3, performance exhibits a distinct inverted V-shaped trend, peaking at  $r = 8$ .

Notably, lower compression ratios ( $r=2, 4$ ) underperform compared to  $r=8$ , suggesting that excessive semantic detail may overwhelm the sequence model and dilute important information. Conversely, overly aggressive compression ( $r=16$ ) creates an information bottleneck, causing significant performance drops. Thus,  $r=8$  serves as an optimal semantic filter, balancing information density with inference efficiency.

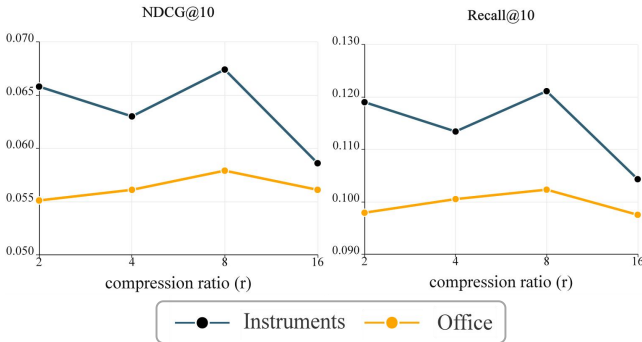


**Figure 3: Impact of compression ratio  $r$  on recommendation performance.**

**3.4.2 Effectiveness of Decoupling Strategy.** To verify that the gains stem from distilling high-resolution inputs rather than merely the model architecture, we compare ACERec against a *Short-digit OPQ* baseline. Crucially, both models feed the **same number of tokens** into the recommender (e.g.,  $k=4$ ), ensuring identical inference costs. The difference lies in the source: ACERec distills them from a long sequence ( $m=32$ ), whereas the baseline generates them directly via OPQ ( $m=4$ ).

As illustrated in Figure 4, ACERec demonstrates a dominant advantage over the direct short tokenization. Quantitatively,

ACERec achieves an impressive average improvement of 44.48% in Recall@10 and 56.91% in NDCG@10 across the datasets. This substantial performance gap provides strong empirical evidence for the necessity of our decoupling strategy. We attribute the inferiority of the baseline to the inherent *attribute entanglement* of short OPQ codes. Compressing high-dimensional item features into a mere 4 discrete tokens forces unrelated attributes (e.g., brand, category, color) to share the same subspace, leading to severe *hash collisions* where distinct items map to identical codes. In contrast, ACERec leverages long semantic IDs ( $m=32$ ) to first disentangle these features into fine-grained subspaces. The ATM then performs a “soft compression” in the continuous latent space, acting as a semantic sieve that preserves salient attributes while filtering out noise. The significant improvement in NDCG confirms that distilling high-fidelity semantics in continuous space is far more effective than rigid low-resolution quantization, even under the same computational budget.

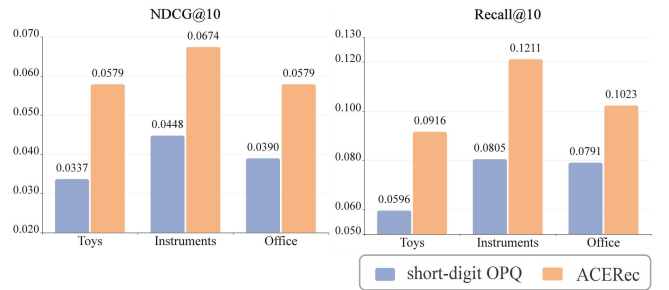


**Figure 4: Performance comparison between ACERec and short-digit OPQ baseline. Both models use the same input length for the recommender.**

### 3.5 Further Analysis

**3.5.1 Robustness on Cold-Start Items.** To assess robustness under cold-start, we bucket test items by their occurrence frequency in the training set:  $[0, 5]$ ,  $[6, 10]$ ,  $[11, 15]$ , and  $[16, 20]$ . As shown in Figure 5, ACERec consistently outperforms all baselines across every frequency interval, maintaining a substantial lead even as interaction sparsity varies. In the extreme-sparsity bucket (e.g.,  $[0, 5]$ ), TIGER and RPG degrade to near-zero performance, as they struggle to establish transferable semantic vocabulary from minimal interaction items. In contrast, ACERec remains competitive, indicating stronger generalization by effectively utilizing interacted item semantics. Moreover, as item frequency increases (e.g.,  $[16, 20]$ ), ACERec further widens the gap, demonstrating stable gains beyond the coldest regime. We attribute this robustness to the synergy of ATM and ISA: ATM distills informative semantics from long OPQ tokens, and ISA aligns the learned intent with item-level semantics, reducing reliance on scarce collaborative signals and enabling more precise retrieval of infrequent items. Additional cold-start results are provided in Appendix C.3.

**3.5.2 Inference Efficiency vs. Effectiveness.** We evaluate the trade-off between inference throughput (samples/s) and NDCG@10 on the Toys dataset (Figure 6). While autoregressive models like

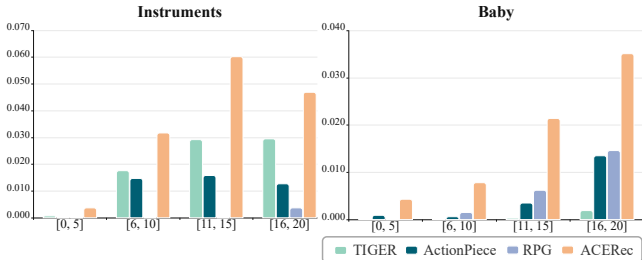


Figure 5: Cold-start analysis on Instruments and Baby datasets, with NDCG@10 as performance metric.

ActionPiece and TIGER are hindered by costly beam search, and RPG is bottlenecked by iterative graph decoding, ACERec achieves an average speedup of 2.2 $\times$  over them. Notably, when TIGER is configured with the same number of tokens (e.g., 4) for the recommender, ACERec exhibits a faster inference rate due to its parallel decoding nature, while simultaneously attaining the best overall performance. These advantages in speed and ranking are directly attributed to our ATM-based decoupling mechanism, which successfully exploits fine-grained semantic sequences through an efficient parallel framework, effectively bridging the gap between representational richness and inference throughput.

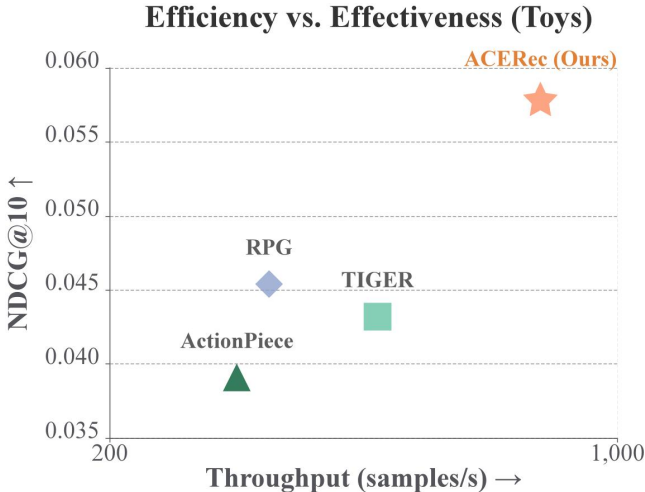


Figure 6: Inference Efficiency and Recommendation Performance on Toys Dataset.

## 4 RELATED WORK

### 4.1 Item ID-based Sequential Recommendation

Sequential recommendation has evolved significantly, from early methods based on Markov Chains [26] that capture local transitions to neural architectures such as RNNs [9, 18, 34] and CNNs [28] designed for non-linear dependency modeling. Currently, Transformer-based models like SASRec [16] and BERT4Rec [27] achieve the state-of-the-art performance by leveraging self-attention to capture complex, long-range dependencies.

Despite their success, these methods predominantly operate in an item ID-based paradigm, where items are treated as atomic, unique identifiers. This approach faces two fundamental challenges: (1) *Scalability*: the embedding table size scales linearly with the catalog, incurring prohibitive memory overhead in large-scale systems; (2) *Information Isolation*: arbitrary IDs lack intrinsic semantic structure, which prevents models from effectively transferring knowledge across items or generalizing to cold-start scenarios where interaction data is sparse [38]. While some methods incorporate side information as auxiliary features [36], they do not fundamentally resolve the retrieval bottleneck inherent in the ID-centric framework.

### 4.2 Generative Sequential Recommendation

To overcome the limitations of item ID-based retrieval, generative recommendation [7, 25] reformulates recommendation as a sequence-to-sequence task over discrete semantic IDs. This paradigm enables knowledge transfer across items via a shared vocabulary but faces a trade-off between input resolution and efficiency. RQ-based models [20, 25] use hierarchical codes but are confined to short sequences (e.g., 4 tokens) due to their serial decoding bottleneck. Conversely, OPQ-based methods [11, 12] leverage orthogonal subspaces to support parallel prediction and expressive long IDs (e.g., 32 tokens) to capture fine-grained item attributes.

However, directly modeling long sequences is computationally prohibitive due to quadratic attention complexity. Existing solutions manage sequence length via rigid pooling, which inevitably causes “semantic blurring” by conflating distinct subspace attributes. ACERec addresses this dilemma by decoupling tokenization granularity from sequential modeling, effectively reconciling representational resolution with inference efficiency.

### 4.3 Intent Learning for Recommendation

User interactions are driven by latent intents that represent high-level preferences. To capture these factors, early research employed multi-interest networks like MIND [17] and ComiRec [3] to extract multiple interest embeddings via dynamic routing or self-attention. The evolution of intent learning is deeply rooted in disentangled representation learning, which aims to decouple various latent factors, such as brand preference or price sensitivity, that drive user decisions. This field has recently shifted toward contrastive intent learning, where ICLRec [4] employs K-means clustering and contrastive objectives to discover latent intent, and ELCRec [21] further unifies clustering and representation learning within an end-to-end architecture.

However, a significant gap remains: existing intent learning frameworks are predominantly tethered to the item-ID paradigm, while current semantic ID-based generative methods focus on digit-level reconstruction. The former inherits the scalability and cold-start limitations, whereas the latter often overlooks global semantic coherence by over-prioritizing fine-grained token prediction. ACERec bridges this gap by unifying token reconstruction with item-wise intent alignment. Instead of relying solely on token-wise supervision, we employ a dual-objective strategy that optimizes for both high-precision sequence generation and semantic consistency.

This approach ensures that the captured user preference is both bit-accurate and semantically grounded.

## 5 CONCLUSION

In this work, we proposed ACERec, a novel framework that resolves the “granularity mismatch” dilemma in generative recommendation by decoupling the tokenization resolution from the recommendation process. At the architectural level, we introduced the ATM, a content-adaptive mechanism that distills fine-grained semantic tokens (e.g., length 32) into compact latents (e.g., length 4). This design effectively filters redundancy while preserving critical item details in a continuous latent space. To govern the prediction process, we devised a dedicated Intent Token as the dynamic anchor and proposed a dual-granularity optimization strategy. By combining fine-grained MTP with the item-wise ISA objective, ACERec ensures that the learned user intent captures both precise token details and salient semantic features. Extensive experiments across multiple datasets demonstrate that ACERec consistently outperforms state-of-the-art discriminative and generative baselines. Meanwhile, ACERec shows robustness in cold-start scenarios, effectively preventing the model collapse observed in existing ID-based methods under extreme sparsity.

## REFERENCES

[1] Prabhat Agarwal, Anirudhan Badrinath, Laksh Bhasin, Jaewon Yang, Edoardo Botta, Jiajing Xu, and Charles Rosenberg. 2025. Pinrec: Outcome-conditioned, multi-token generative retrieval for industry-scale recommendation systems. *arXiv preprint arXiv:2504.10507* (2025).

[2] Yoshua Bengio and Jean-Sébastien Sénelac. 2008. Adaptive importance sampling to accelerate training of a neural probabilistic language model. *IEEE Transactions on Neural Networks* 19, 4 (2008), 713–722.

[3] Yukuo Cen, Jianwei Zhang, Xu Zou, Chang Zhou, Hongxia Yang, and Jie Tang. 2020. Controllable multi-interest framework for recommendation. In *Proceedings of the 26th ACM SIGKDD international conference on knowledge discovery & data mining*. 2942–2951.

[4] Yongjun Chen, Zhiwei Liu, Jia Li, Julian McAuley, and Caiming Xiong. 2022. Intent contrastive learning for sequential recommendation. In *Proceedings of the ACM web conference 2022*. 2172–2182.

[5] Matthijs Douze, Alexandre Guizha, Chengqi Deng, Jeff Johnson, Gergely Szilvassy, Pierre-Emmanuel Mazaré, Maria Lomeli, Lucas Hosseini, and Hervé Jégou. 2025. The faiss library. *IEEE Transactions on Big Data* (2025).

[6] Tiezheng Ge, Kaiming He, Qifa Ke, and Jian Sun. 2013. Optimized product quantization. *IEEE transactions on pattern analysis and machine intelligence* 36, 4 (2013), 744–755.

[7] Shijie Geng, Shuchang Liu, Zuohui Fu, Yingqiang Ge, and Yongfeng Zhang. 2022. Recommendation as language processing (rlp): A unified pretrain, personalized prompt & predict paradigm (p5). In *Proceedings of the 16th ACM conference on recommender systems*. 299–315.

[8] Fabian Gloclekle, Badi Youbi Idrissi, Baptiste Rozière, David Lopez-Paz, and Gabriel Synnaeve. 2024. Better & faster large language models via multi-token prediction. *arXiv preprint arXiv:2404.19737* (2024).

[9] Balázs Hidasi, Alexandros Karatzoglou, Linas Baltrunas, and Domonkos Tikk. 2015. Session-based recommendations with recurrent neural networks. *arXiv preprint arXiv:1511.06939* (2015).

[10] Chris Hokamp and Qun Liu. 2017. Lexically constrained decoding for sequence generation using grid beam search. *arXiv preprint arXiv:1704.07138* (2017).

[11] Yupeng Hou, Zhankui He, Julian McAuley, and Wayne Xin Zhao. 2023. Learning vector-quantized item representation for transferable sequential recommenders. In *Proceedings of the ACM Web Conference 2023*. 1162–1171.

[12] Yupeng Hou, Jiacheng Li, Ashley Shin, Jinsung Jeon, Abhishek Santhanam, Wei Shao, Kaveh Hassani, Ning Yao, and Julian McAuley. 2025. Generating long semantic ids in parallel for recommendation. In *Proceedings of the 31st ACM SIGKDD Conference on Knowledge Discovery and Data Mining* V. 2. 956–966.

[13] Yupeng Hou, Jianmo Ni, Zhankui He, Noveen Sachdeva, Wang-Cheng Kang, Ed H Chi, Julian McAuley, and Derek Zhiyuan Cheng. 2025. ActionPiece: Contextually Tokenizing Action Sequences for Generative Recommendation. *arXiv preprint arXiv:2502.13581* (2025).

[14] Yupeng Hou, An Zhang, Leheng Sheng, Jiancan Wu, Xiang Wang, Tat-Seng Chua, and Julian McAuley. 2025. Towards large generative recommendation: A tokenization perspective. In *Proceedings of the 34th ACM International Conference on Information and Knowledge Management*. 6821–6824.

[15] Hervé Jegou, Matthijs Douze, and Cordelia Schmid. 2010. Product quantization for nearest neighbor search. *IEEE transactions on pattern analysis and machine intelligence* 33, 1 (2010), 117–128.

[16] Wang-Cheng Kang and Julian McAuley. 2018. Self-attentive sequential recommendation. In *2018 IEEE international conference on data mining (ICDM)*. IEEE, 197–206.

[17] Chao Li, Zhiyuan Liu, Mengmeng Wu, Yuchi Xu, Huan Zhao, Pipei Huang, Guoliang Kang, Qiwei Chen, Wei Li, and Dik Lun Lee. 2019. Multi-interest network with dynamic routing for recommendation at Tmall. In *Proceedings of the 28th ACM international conference on information and knowledge management*. 2615–2623.

[18] Jing Li, Pengjie Ren, Zhumin Chen, Zhaochun Ren, Tao Lian, and Jun Ma. 2017. Neural attentive session-based recommendation. In *Proceedings of the 2017 ACM on Conference on Information and Knowledge Management*. 1419–1428.

[19] Lei Li, Yongfeng Zhang, Dugang Liu, and Li Chen. 2024. Large language models for generative recommendation: A survey and visionary discussions. In *Proceedings of the 2024 Joint International Conference on Computational Linguistics, Language Resources and Evaluation (LREC-COLING 2024)*. 10146–10159.

[20] Enze Liu, Bowen Zheng, Cheng Ling, Lantao Hu, Han Li, and Wayne Xin Zhao. 2025. Generative recommender with end-to-end learnable item tokenization. In *Proceedings of the 48th International ACM SIGIR Conference on Research and Development in Information Retrieval*. 729–739.

[21] Yue Liu, Shihao Zhu, Jun Xia, Yingwei Ma, Jian Ma, Xinwang Liu, Shengju Yu, Kejun Zhang, and Wenliang Zhong. 2024. End-to-end learnable clustering for intent learning in recommendation. *Advances in Neural Information Processing Systems* 37 (2024), 5913–5949.

[22] Chen Ma, Peng Kang, and Xue Liu. 2019. Hierarchical gating networks for sequential recommendation. In *Proceedings of the 25th ACM SIGKDD international conference on knowledge discovery & data mining*. 825–833.

[23] Julian McAuley, Christopher Targett, Qinfeng Shi, and Anton Van Den Hengel. 2015. Image-based recommendations on styles and substitutes. In *Proceedings of the 38th international ACM SIGIR conference on research and development in information retrieval*. 43–52.

[24] Jianmo Ni, Gustavo Hernandez Abrego, Noah Constant, Ji Ma, Keith Hall, Daniel Cer, and Yinfei Yang. 2022. Sentence-t5: Scalable sentence encoders from pre-trained text-to-text models. In *Findings of the association for computational linguistics: ACL 2022*. 1864–1874.

[25] Shashank Rajput, Nikhil Mehta, Anima Singh, Raghunandan Hulikal Keshavan, Trung Vu, Lukasz Heldt, Lichan Hong, Yi Tay, Vinh Tran, Jonah Samost, et al. 2023. Recommender systems with generative retrieval. *Advances in Neural Information Processing Systems* 36 (2023), 10299–10315.

[26] Steffen Rendle, Christoph Freudenthaler, and Lars Schmidt-Thieme. 2010. Factorizing personalized markov chains for next-basket recommendation. In *Proceedings of the 19th international conference on World wide web*. 811–820.

[27] Fei Sun, Jun Liu, Jian Wu, Changhua Pei, Xiao Lin, Wenwu Ou, and Peng Jiang. 2019. BERT4Rec: Sequential recommendation with bidirectional encoder representations from transformer. In *Proceedings of the 28th ACM international conference on information and knowledge management*. 1441–1450.

[28] Jiaxi Tang and Ke Wang. 2018. Personalized top-n sequential recommendation via convolutional sequence embedding. In *Proceedings of the eleventh ACM international conference on web search and data mining*. 565–573.

[29] Ashish Vaswani, Noam Shazeer, Niki Parmar, Jakob Uszkoreit, Llion Jones, Aidan N Gomez, Łukasz Kaiser, and Illia Polosukhin. 2017. Attention is all you need. *Advances in neural information processing systems* 30 (2017).

[30] Hao Wang, Wei Guo, Luankang Zhang, Jin Yao Chin, Yufei Ye, Huifeng Guo, Yong Liu, Defu Lian, Ruiming Tang, and Enhong Chen. 2025. Generative large recommendation models: Emerging trends in llms for recommendation. In *Companion Proceedings of the ACM on Web Conference 2025*. 49–52.

[31] Wenjie Wang, Xinyu Lin, Fuli Feng, Xiangnan He, and Tat-Seng Chua. 2023. Generative recommendation: Towards next-generation recommender paradigm. *arXiv preprint arXiv:2304.03516* (2023).

[32] Thomas Wolf, Lysandre Debut, Victor Sanh, Julien Chaumond, Clement Delangue, Anthony Moi, Pierrick Cistac, Tim Rault, Remi Louf, Morgan Funtowicz, et al. 2020. Transformers: State-of-the-art natural language processing. In *Proceedings of the 2020 conference on empirical methods in natural language processing: system demonstrations*. 38–45.

[33] Xinyang Yi, Ji Yang, Lichan Hong, Derek Zhiyuan Cheng, Lukasz Heldt, Aditee Kumthekar, Zhe Zhao, Li Wei, and Ed Chi. 2019. Sampling-bias-corrected neural modeling for large corpus item recommendations. In *Proceedings of the 13th ACM conference on recommender systems*. 269–277.

[34] Zhenrui Yue, Yueqi Wang, Zhankui He, Huimin Zeng, Julian McAuley, and Dong Wang. 2024. Linear recurrent units for sequential recommendation. In *Proceedings of the 17th ACM international conference on web search and data mining*. 930–938.

[35] Neil Zeghidour, Alejandro Luebs, Ahmed Omran, Jan Skoglund, and Marco Tagliasacchi. 2021. Soundstream: An end-to-end neural audio codec. *IEEE/ACM Transactions on Audio, Speech, and Language Processing* 30 (2021), 495–507.

[36] Tingting Zhang, Pengpeng Zhao, Yanchi Liu, Victor S Sheng, Jiajie Xu, Deqing Wang, Guanfeng Liu, Xiaofang Zhou, et al. 2019. Feature-level deeper self-attention network for sequential recommendation. In *IJCAI*. 4320–4326.

[37] Wayne Xin Zhao, Shanlei Mu, Yupeng Hou, Zihan Lin, Yushuo Chen, Xingyu Pan, Kaiyuan Li, Yujie Lu, Hui Wang, Changxin Tian, et al. 2021. Recbole: Towards a unified, comprehensive and efficient framework for recommendation algorithms. In *Proceedings of the 30th ACM international conference on information & knowledge management*. 4653–4664.

[38] Kun Zhou, Hui Wang, Wayne Xin Zhao, Yutao Zhu, Sirui Wang, Fuzheng Zhang, Zhongyuan Wang, and Ji-Rong Wen. 2020. S3-rec: Self-supervised learning for sequential recommendation with mutual information maximization. In *Proceedings of the 29th ACM international conference on information & knowledge management*. 1893–1902.

## A EXPERIMENTAL SETTING DETAILS

### A.1 Baseline Details

We compare ACERec with nine state-of-the-art baselines. These methods are categorized into two groups: (1) **item ID-based methods**, which rely on unique item (or improved by feature) indices, and (2) **semantic ID-based methods**, which leverage item content (e.g., brand and price). The detailed description for these baselines are as follows:

- **HGN** [22]: utilizes a hierarchical gating network to capture both long-term and short-term user interests from interaction sequences.
- **SASRec** [16]: employs a self-attentive Transformer decoder to model sequential dynamics and predict the next item.
- **S<sup>3</sup>-Rec** [38]: utilizes mutual information maximization to pre-train the model with correlations among items, attributes, and subsequences.
- **ICLRec** [4]: learns latent user intents via clustering and contrastive learning within an Expectation-Maximization framework.
- **ELCRec** [21]: unifies behavior representation and clustering into an end-to-end framework to efficiently capture latent user intents.
- **TIGER** [25]: quantizes items into hierarchical semantic IDs via RQ-VAE and autoregressively generates the next item’s tokens.
- **ActionPiece** [13]: proposes context-aware tokenization by representing actions as feature sets and merging co-occurring patterns.
- **ETEGRec** [20]: jointly optimizes the item tokenizer and the generative recommender using multi-view alignment objectives.
- **RPG** [12]: utilizes OPQ to construct long semantic IDs and adopts a MTP objective for parallel generation.

### A.2 Implementation Details

**Baselines.** To ensure a rigorous comparison, we adopt the reported results from Rajput *et al.* [25] for HGN, SASRec, S<sup>3</sup>-Rec, and TIGER on the Sports, Beauty, and Toys datasets. For all other datasets and baselines, we reproduce the results using their official implementations or the RecBole library [37], carefully tuning hyperparameters as suggested in their original papers.

**Unified Semantic Encoder.** To ensure a fair comparison, we consistently employ the sentence-t5-base [24] as the universal semantic encoder for *all* semantic ID-based methods, ensuring that any performance gains are attributed to our proposed architecture rather than superior raw semantic embeddings. We use the FAISS library [5] to implement OPQ.

**ACERec.** We implement our method using HuggingFace transformers [32] and align the model configuration with RPG [12] for fair comparison. Specifically, we utilize a 2-layer Transformer [29] decoder with an embedding dimension of  $d=448$ , a feed-forward network dimension of 1024, and 4 attention heads. Regarding the semantic ID length  $m$ , we focus on  $m \in \{32, 64\}$  to fully leverage the expressive power of long sequences, while the default compression ratio is 8. The codebook size  $M$  is set to 256. Key hyperparameters are configured as follows: the popularity debiasing

strength  $\beta = 0.02$ , the MTP prediction temperature  $\gamma = 0.03$ , and the ISA alignment temperature  $\tau = 0.07$ .

All experiments were conducted on a single NVIDIA RTX 6000 Ada GPU (48GB). To manage the search space efficiently, we adopt a *two-stage tuning protocol*. First, we fix the ISA weight  $\lambda = 0.01$  and perform a grid search over the learning rate in  $\{0.003, 0.005, 0.01\}$  and batch size in  $\{64, 128, 256\}$ , totaling 9 hyperparameter settings. Second, based on the optimal configuration from the first stage, we fine-tune  $\lambda$  with  $\{0.03, 0.05, 0.07, 0.1\}$ . This results in a total of 13 experimental runs per dataset. For inference, unlike baselines that depend on beam search [25] or decoding parameters [12], ACERec requires no generation strategy tuning; we simply load the best checkpoint based on validation NDCG@10 performance and perform holistic candidate scoring.

**Table 5: Statistics of the processed datasets. “Avg.  $t$ ” denotes the average number of interactions per input sequence.**

Datasets	#Users	#Items	#Interactions	Avg. $t$
<b>Sports</b>	18,357	35,598	260,739	8.32
<b>Beauty</b>	22,363	12,101	176,139	8.87
<b>Toys</b>	19,412	11,924	148,185	8.63
<b>Instruments</b>	1,430	901	10,261	7.18
<b>Office</b>	4,906	2,421	53,258	10.86
<b>Baby</b>	19,446	7,051	160,792	8.27

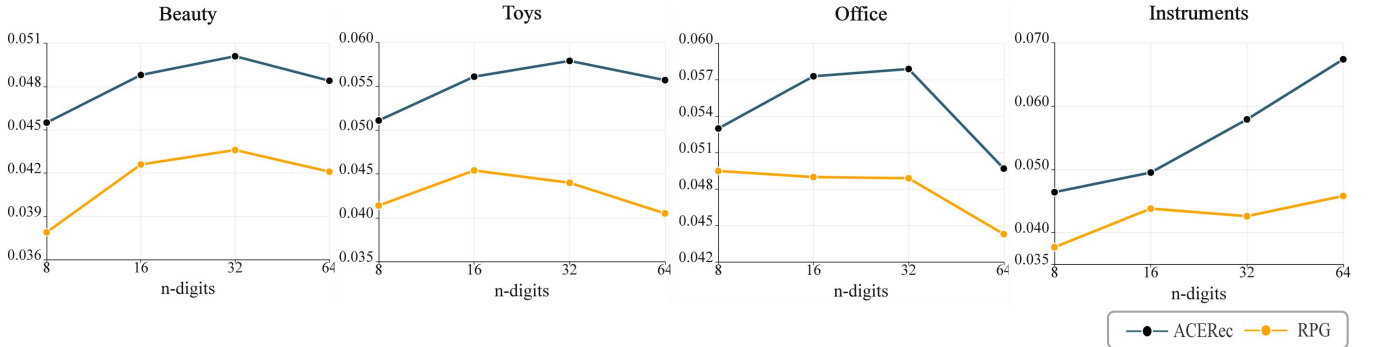
### A.3 Dataset Statistics

The experiments are conducted on six public benchmark datasets from the Amazon product reviews collection [23], spanning diverse domains: **Sports**, **Beauty**, **Toys**, **Instruments**, **Office**, and **Baby**. These datasets comprise user reviews and item metadata collected between May 1996 and July 2014.

The data has been processed following standard evaluation protocols for sequential recommendation: item sequences for each user are sorted chronologically by timestamps, and users with fewer than five interactions are excluded to ensure sufficient context. During the training phase, the length of user historical sequences is truncated to the 50 most recent interactions to maintain computational efficiency. The final statistics of the processed datasets are summarized in Table 5.

## B PROCEDURE OF ACEREC

In this section, we provide the detailed algorithmic procedures for both the training and inference phases of ACERec. Algorithm 1 outlines the end-to-end training flow, systematically integrating fine-grained tokenization via OPQ and attentive token merging, latent sequence modeling with step-wise causal masking, and the dual-granularity optimization strategy. Algorithm 2 presents the inference phase, utilizing our holistic candidate scoring strategy. Unlike autoregressive approaches, it demonstrates how ACERec achieves efficient exact retrieval by computing subspace probabilities in parallel and performing vectorized score aggregation over the entire item catalog.

Figure 7: NDCG@10 performance under different digit length  $m$ .**Algorithm 1** Training Procedure of ACERec

**Input:** User sequences  $\mathcal{D} = \{(\mathcal{S}_u, i_{tgt})\}$ , OPQ codebooks  $\{C^{(k)}\}$ .  
**Output:** Trained Model parameters  $\Theta$ .

- 1: **Initialize** parameters  $\Theta$  with random values.
- 2: **while** not converged **do**
- 3:     **for** each sample  $(\mathcal{S}_u, i_{tgt})$  in  $\mathcal{D}$  **do**
- 4:         // Phase 1: Token Compression
- 5:         **for** each item  $i_t \in \mathcal{S}_u$  **do**
- 6:             Generate queries  $Q_t$  and intent  $h_t$  by Equation (1).
- 7:             Merge latent tokens  $Z_t$  via Equation (2).
- 8:             Form composite block  $\tilde{Z}_t = [Z_t; h_t]$ .
- 9:         // Phase 2: Sequence modeling
- 10:         Construct Step-wise Causal Mask  $M$ .
- 11:         Aggregate Intent  $h_{pred} \leftarrow \text{Decoder}([\tilde{Z}_1, \dots, \tilde{Z}_L], M)$ .
- 12:         // Phase 3: Dual-Granularity Optimization
- 13:         Compute MTP Loss  $\mathcal{L}_{MTP}$  by Equation (4).
- 14:         Compute ISA Loss  $\mathcal{L}_{ISA}$  by Equation (6).
- 15:          $\mathcal{L} \leftarrow \mathcal{L}_{MTP} + \lambda \mathcal{L}_{ISA}$ .
- 16:         Update  $\Theta \leftarrow \Theta - \eta \nabla \mathcal{L}$ .

**Algorithm 2** Inference via Holistic Candidate Scoring

**Input:** Trained model  $\Theta$ , User history  $\mathcal{S}_u$ , Item set  $\mathcal{I}$ .  
**Output:** Top- $K$  recommendations.

- 1: // Step 1: Contextualized Encoding
- 2: **for** each item  $i_t \in \mathcal{S}_u$  **do**
- 3:     Generate latents  $Z_t$  and intent  $h_t$  by Equation (1) and (2).
- 4:     Form composite block  $\tilde{Z}_t = [Z_t; h_t]$ .
- 5:     Construct Step-wise Causal Mask  $M$ .
- 6:     Aggregate Intent  $h_{pred} \leftarrow \text{Decoder}([\tilde{Z}_1, \dots, \tilde{Z}_L], M)$ .
- 7:     // Step 2: Parallel Subspace Matching
- 8:     Project  $h_{pred}$  into  $m$  subspace queries  $\{h^{(1)}, \dots, h^{(m)}\}$ .
- 9:     **for** digit  $k = 1$  to  $m$  **in parallel** **do**
- 10:         Compute logits  $P[k, \cdot]$  by Equation (8).
- 11:     // Step 3: Vectorized Score Gathering
- 12:     **Gather** scores  $S \in \mathbb{R}^{|\mathcal{I}|}$  for all items  $j \in \mathcal{I}$  by Equation (9).
- 13:     **return** Top- $K$  indices from  $S$ .

**C ADDITIONAL EXPERIMENTS RESULTS****C.1 Scalability of Semantic ID Lengths  $m$** 

The semantic ID length  $m$  governs the granularity of item representation. To analyze its impact, we vary  $m \in \{8, 16, 32, 64\}$  (fixing ACERec’s compression ratio at  $r = 8$ ). We compare the NDCG@10 performance of ACERec against RPG [12] on four datasets, as shown in Figure 7.

First, ACERec consistently outperforms RPG across all granularity settings, demonstrating better adaptability to different representation resolutions. Second, regarding scalability, RPG exhibits early saturation or even degradation at larger  $m$  (e.g., on Office and Beauty), suggesting that rigid mean pooling struggles to distill informative signals from long sequences without introducing noise. In contrast, ACERec shows robust improvements as  $m$  increases from 8 to 32, as our attentive merging mechanism adaptively emphasizes salient semantic features while suppressing redundant information. Finally, we observe that  $m=32$  serves as a generic “sweet spot”, yielding optimal performance for Beauty, Toys, and Office. An exception is the Instruments dataset, which continues to benefit from finer granularity and peaks at  $m = 64$ . Consequently, we adopt  $m=64$  for Instruments and  $m = 32$  for the remaining datasets in our main experiments.

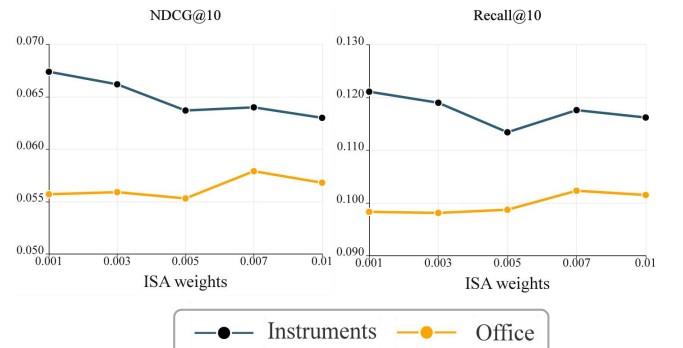


Figure 8: Performance comparison of different loss coefficients.

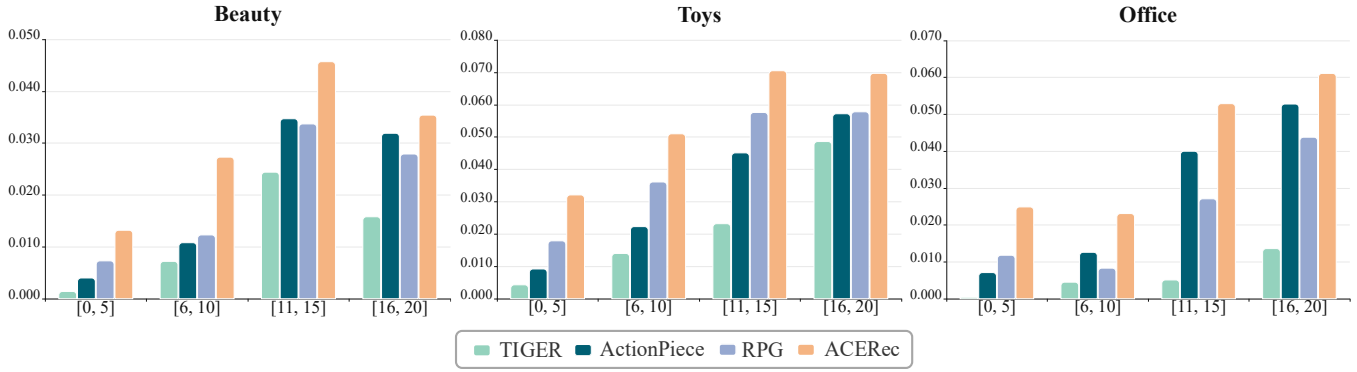


Figure 9: Additional cold-start performance (NDCG@10) on Beauty, Toys, and Office datasets.

## C.2 Sensitivity of ISA Weight $\lambda$

To analyze how the strength of  $\mathcal{L}_{\text{ISA}}$  affects performance, we vary the loss weight  $\lambda$  in the range  $\{0.001, 0.003, 0.005, 0.007, 0.01\}$  on the Instruments and Office datasets. The results are illustrated in Figure 8. We observe that ACERec exhibits robustness to variations in  $\lambda$  across the investigated range. This suggests that the ISA serves as a stable regularizer that complements the token-level supervision. Nonetheless, each dataset exhibits distinct preferences, so we tune  $\lambda$  to achieve optimal performance.

## C.3 Additional Cold-Start Analysis

To further substantiate the robustness of ACERec, we present a detailed breakdown of item frequency distributions in Table 6 and extend the cold-start analysis (Section 3.5.1 in the main text) to the Beauty, Toys, and Office datasets (Figure 9) with the same partition protocol.

**Prevalence of Long-Tail Items.** The statistics in Table 6 reveal a pervasive long-tail distribution across all domains. Notably, items in the extreme sparsity bucket ( $[0, 5]$ ) constitute a substantial portion of the test set, ranging from 19.30% (Baby) to as high as 38.84% (Instruments). When combined with the  $[6, 10]$  bucket, sparse items account for nearly half of the catalog in most datasets. This underscores that cold-start performance is not merely an edge case but a dominant factor determining overall recommendation effectiveness.

Table 6: Distribution of test items based on their interaction frequency in the training set. The values indicate the percentage of test items falling into each sparsity bucket.

Dataset	Item Frequency Buckets				
	$[0, 5]$	$[6, 10]$	$[11, 15]$	$[16, 20]$	$[21, \infty)$
<b>Sports</b>	27.98%	19.15%	10.66%	7.26%	34.95%
<b>Beauty</b>	27.71%	19.05%	11.35%	6.84%	35.05%
<b>Toys</b>	32.19%	20.66%	11.47%	7.49%	28.19%
<b>Instruments</b>	38.84%	24.28%	12.53%	5.67%	18.68%
<b>Office</b>	28.38%	15.11%	9.42%	6.79%	40.30%
<b>Baby</b>	19.30%	15.10%	10.32%	8.05%	47.23%

**Performance Consistency.** As shown in Figure 9, ACERec exhibits consistent robustness on three additional datasets, aligning with the observations in the main text. Crucially, in the high-prevalence  $[0, 5]$  bucket, ACERec significantly outperforms baselines—nearly doubling RPG’s performance on Beauty and Office. Given that 27.71% of Beauty and 28.38% of Office items fall into this category, this gain translates to a meaningful real-world impact. This strongly confirms that our model design effectively prevents model collapse and enables stable knowledge transfer.

## C.4 Interplay between Semantic Resolution and Latent Capacity

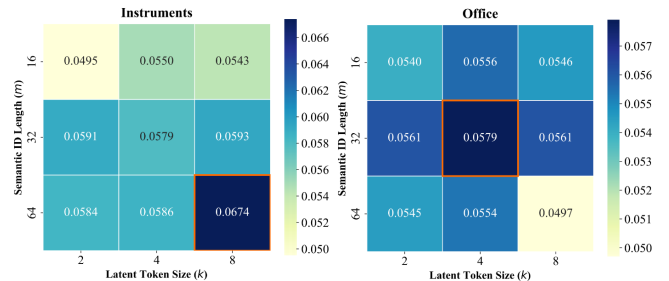
Figure 10: NDCG@10 Performance Comparison with varying digit length  $m$  and compressed latents size  $k$ .

Figure 10 illustrates the performance impact of varying the input semantic length  $m$  and latent size  $k$ . Crucially, we observe that input resolution dominates latent capacity: the configuration ( $m = 32, k = 4$ ) consistently outperforms ( $m = 16, k = 8$ ) across both datasets. This confirms that a bottleneck in raw semantic fidelity cannot be compensated for by simply increasing the number of latent tokens; fine-grained input is a prerequisite for superior recommendation performance. Furthermore, the optimal granularity correlates with domain complexity. For Instruments, performance scales monotonically with both  $m$  and  $k$ , eventually peaking at the highest resolution ( $m = 64, k = 8$ ). In contrast, Office achieved suboptimal performance at  $m = 16$  and saturated performance at  $m = 32$ .

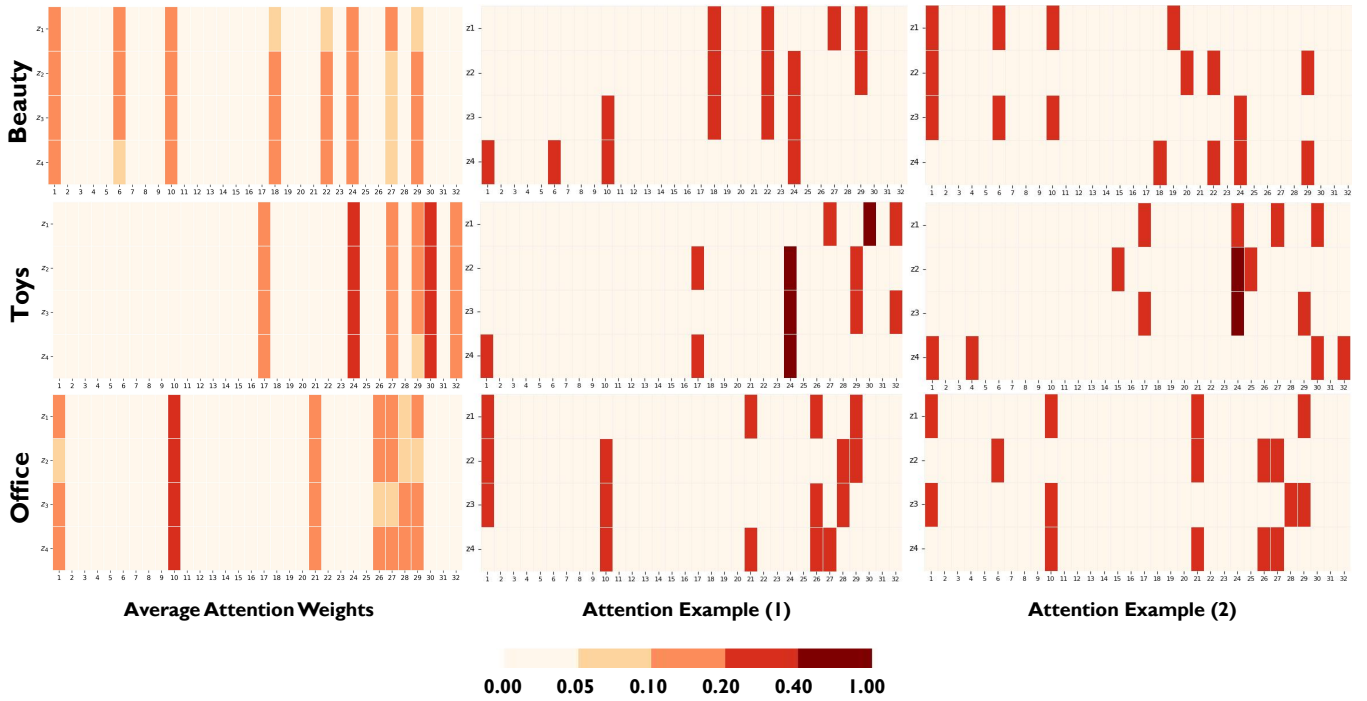


Figure 11: Visualization of ATM compression.

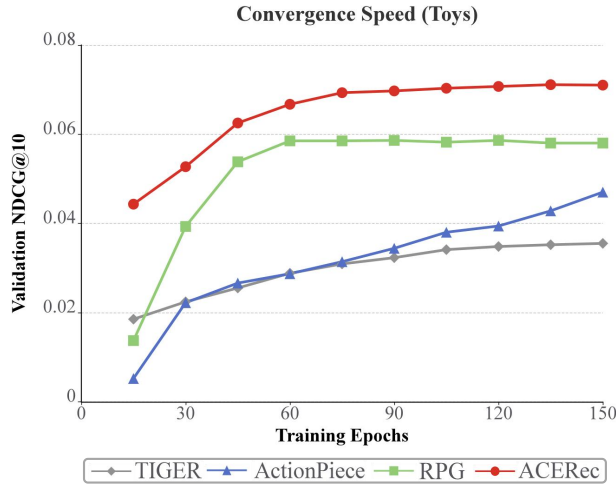


Figure 12: Training Dynamics and Convergence Rate on Toys Dataset.

### C.5 Visualization of Adaptive Semantic Distillation

Figure 11 visualizes the ATM attention weights, offering insights into how the model bridges high-fidelity inputs ( $m = 32$ ) and compact latent states ( $k = 4$ ).

First, the global average patterns (Col. 1) reveal a “sparse-yet-focused” activation mechanism. ATM automatically identifies domain-specific “hotspot” subspaces (e.g., indices 24 and 30 in Toys) that likely encode dominant attributes, while assigning near-zero

weights to less informative regions. This confirms that ATM acts as a semantic distiller, extracting high-purity signals rather than performing rigid pooling and diluting distinctive features.

Second, the individual examples (Cols. 2 & 3) demonstrate ATM’s *content-adaptive* nature. While adhering to the global structure, distinct items trigger different semantic subspaces. For instance, in Beauty, Example 1 focuses on index 27, whereas Example 2 shifts attention to index 19. This proves that ATM performs dynamic, on-demand sampling: distinct items require access to different subspaces to be fully described. A static short code (e.g.,  $m = 4$ ) would forcibly collapse these distinct features, leading to attribute entanglement.

### C.6 Comparison of Convergence Rate

We further investigate the learning efficiency and training stability of ACERec by tracking the validation NDCG@10 among 150 training epochs on Toys. As shown in Figure 12, ACERec converges substantially faster and reaches a higher plateau than other generative baselines: its NDCG@10 surpasses 0.06 within only 40 epochs and consistently stabilizes around 0.071 after 70 epochs. In contrast, RPG improves rapidly at the beginning but saturates early at approximately 0.058, potentially due to the limited expressive power of its mean-pooling architecture. Meanwhile, ActionPiece and TIGER exhibit much slower progress and remain below 0.046 and 0.035 even after 150 epochs, reflecting the optimization difficulties. Overall, the training trajectory indicates that ACERec is both more sample-efficient (faster rise) and achieves a better performance ceiling (higher plateau), suggesting more effective optimization over long semantic-ID representations.